Isoelectronic study of double-electron capture in slow ion-atom collisions

R. Hutton* and D. Schneider
High Temperature Plasma Division, Lawrence Livermore National Laboratory, P. O. Box 808, L-421, Livermore, California 94550

M. H. Prior
Chemical Sciences Division, Lawrence Berkeley Laboratory, Berkeley, California 94720
(Received 10 December 1990)

We report studies of double-electron transfer in slow collisions ($v \approx 0.2$–0.4 a.u.) of the F-like (nine-electron) ions Si^{5+}, Ar^{9+}, Sc^{12+}, Ti^{13+}, Fe^{17+}, and Cu^{20+} with He atoms. The transfer populates doubly excited states of the Na sequence (eleven electrons) of these elements that we study via the subsequent electron emission using high-resolution Auger spectroscopic techniques. Comparison is made to spectra that are formed by single-electron capture by Ne-like (ten-electron) ions in the $2p^5 3s\ ^3P_{0,2}$ metastable levels. Non-Coulomb (Breit interaction) Auger decay of the Na-like metastable level $2p^5 3s 3p\ ^4D_{7/2}$ forms a prominent line in many of these spectra.

INTRODUCTION

Due to the development of a number of new sources of highly charged ions, the study of slow ion-atom collisions has been essentially revitalized. Highly charged ion-atom collisions have been studied for many years using fast beams from high-energy accelerators, i.e., in the regime where the kinetic energy of the projectile always dominates over the potential energy involved in the collision [1]. Modern types of ion sources allow the production of highly charged ions with considerably less kinetic energy than those from accelerators. This is done by reversing the process of fast ions colliding on slow electrons (e.g., in a foil) and using fast electrons to ionize the species of interest, typically at near room temperature [2]. Examples of such ion sources are the electron cyclotron resonance (ECR) sources [3], electron-beam ion sources (EBIS) [4], and the recent extraction of very highly charged ions from an electron-beam ion trap (EBIT) [5]. By using such sources, an inadequately explored energy region in ion-atom collisions becomes accessible both for sophisticated spectroscopic studies as well as for the study of excitation-capture processes. Reference [6] gives a recent review of low-energy ion-atom collisions.

This work reports experiments involving highly charged ion beams extracted from the Lawrence Berkeley Laboratory Electron Cyclotron Resonance (LBL ECR) ion source [7]. The experiments concerned the production of Na-like core-excited configurations by electron capture from He target atoms. The elements used in this work are Si, Ar, Ti, Sc, Fe, and Cu. For a number of these elements, the Na-like core-excited configurations were populated in two different ways, i.e., double-electron capture to F-like ($2p^5$) beams or single-electron capture to the $2p^5 3s$ metastable fraction of the corresponding Ne-like beams. In the single-capture case we make use of the well-developed semiclassical over-barrier model [8] to describe the collision. The main aim of this work is to show systematic trends in the double-electron-capture mechanism for F-like beams colliding on He.

EXPERIMENT

The experiments to be discussed here have been conducted using highly charged F- and Ne-like ions extracted from the LBL ECR ion source. In all cases the ion beams were extracted from the source at 10-kV extraction potential (i.e., beam velocities of 0.24–0.36 a.u.). After charge-mass analysis the ions were directed into one of the two beam lines used for slow ion-atom collision studies ($v \leq 1$ a.u.); see Fig. 1 and Ref. [9]. One of the beam lines has a zero-degree tandem spectrometer consisting of an electrostatic 45° parallel-plate analyzer and a commercial McPherson spherical sector electron analyzer. This system has been described in earlier works [10], [11]. The second beam line has a more general purpose scattering chamber. Particular features of this chamber include a rotatable 45° electron analyzer and provide for the placement of a number of gas jets at varying distances along the beam for time-of-flight studies.

The target cell in the tandem spectrometer line consists of an outer and inner cell insulated from each other [12]. The application of a biasing voltage to the inner cell shifts the energy of electrons produced inside the cell (prompt decays). This also allows the measurement of low-energy electrons by shifting them to energies above the detection threshold (~ 5 eV). A demonstration of the cell-biasing technique in distinguishing Auger lines from allowed and forbidden transitions is shown in Fig. 2 (see Ref. [11] for more detail). This technique was used extensively in these experiments.

In each of the beam lines the ion beam is shaped by two sets of adjustable (four-jaw) collimators separated by approximately 1 m. The upstream collimator is used to define a beam with an approximate size of 2×2 mm^2,

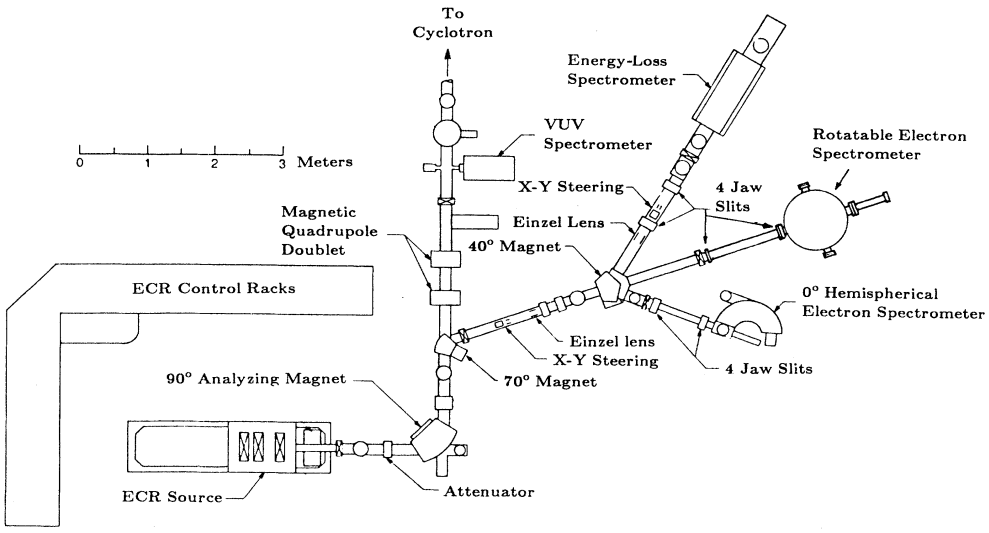

FIG. 1. This figure shows the general layout of the atomic physics facility at the LBL ECR ion source. After mass-charge analysis through a 90° magnet, the beam is directed towards the atomic physics beam line by a 70° magnet. The beam line is then divided into three experimental lines by a 40° magnet. Two of these beam lines have been used in these experiments.

while the second collimator is used to eliminate slit scattered particles. This degree of beam collimation reduces the background electron rate due to scattered ion beam to minimal levels. The use of the large volume McPherson hemispherical analyzer also reduces background due to scattered electrons often to negligible levels.

The experiments were run with typical pressures of about 5×10^{-8} Torr in the beam transport lines, 1×10^{-7} Torr in the target chamber, and gas cell pressures ranging from 0.1 to 1.5 mTorr. The target cell pressure was monitored by a capacitance manometer and regulated by an automatic leak valve; the target gas was always He. The dwell time in each energy channel was normalized to a constant amount of integrated beam current collected in a Faraday cup.

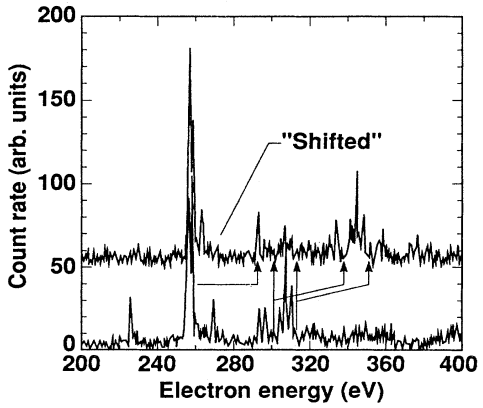

FIG. 2. The effect of the cell bias voltage is demonstrated for metastable (i.e., long-lived) levels. The $2p^5 3s 3p\ ^4D_{7/2}$ Auger decay line is left unaffected by the -40 V bias used to obtain the "shifted" spectrum. The feature at around 302 eV appears to have some metastability as shown by the arrows. The $3s3d\ ^4F_{9/2}$ level is known to be 49.9 eV above the $3s3p\ ^4D_{7/2}$ level [28].

RESULTS

Auger spectra have been recorded for the Na-like final-state projectile ions Si^{3+}, Ar^{7+}, Sc^{10+}, Ti^{11+}, Fe^{15+}, and Cu^{18+}. An overview of measured spectra for Si, Ar, Ti, and Fe is shown in Fig. 3 after transformation to the emitter frame. In those cases where it was possible (i.e., Si, Ar, and ^{48}Ti), the Na-like final states have been produced by both double-electron capture to F-like beams and single-electron capture to Ne-like beams. The Ne-like beams of Fe^{16+} and Cu^{19+} were found to contain little or no $2p^5 3s\ ^3P_{0,2}$ metastable components because the lifetime of these levels is too short to survive the transit time from the source to the spectrometer. The metastable levels in Ne-like Sc^{11+} and $^{47}Ti^{12+}$ may be quenched by the hyperfine interaction. A schematic energy-level scheme for some of the $2p^5 nln'l'$ configurations is shown in Fig. 4.

F-LIKE PROJECTILES

The ground-state configuration of F-like ions is $2p^5$ and there are no long-lived (metastable) excited configurations. Single-electron capture populates nonautoionizing configurations, i.e., $2p^5 nl$, which are the normal Ne-like excited configurations. However, double-electron capture to the F-like beam will populate Auger levels. This process can occur by two independent mechanisms: (i) two independent single-electron-capture col-

lisions, the first leaving the ion in one of the Ne-like metastable levels ($2p^5 3s\ ^3P_{0,2}$) either directly or via cascading; (ii) double-electron capture in a single collision. These two processes can be distinguished by their target pressure dependence. A study of Auger line intensity versus target pressure was presented in Ref. [13] for the collision system Ar^{9+} on He. Similar pressure-dependence studies were also done for the elements presented here, e.g., Fig. 5 shows the pressure variation for 130-keV Ti^{13+} colliding on He.

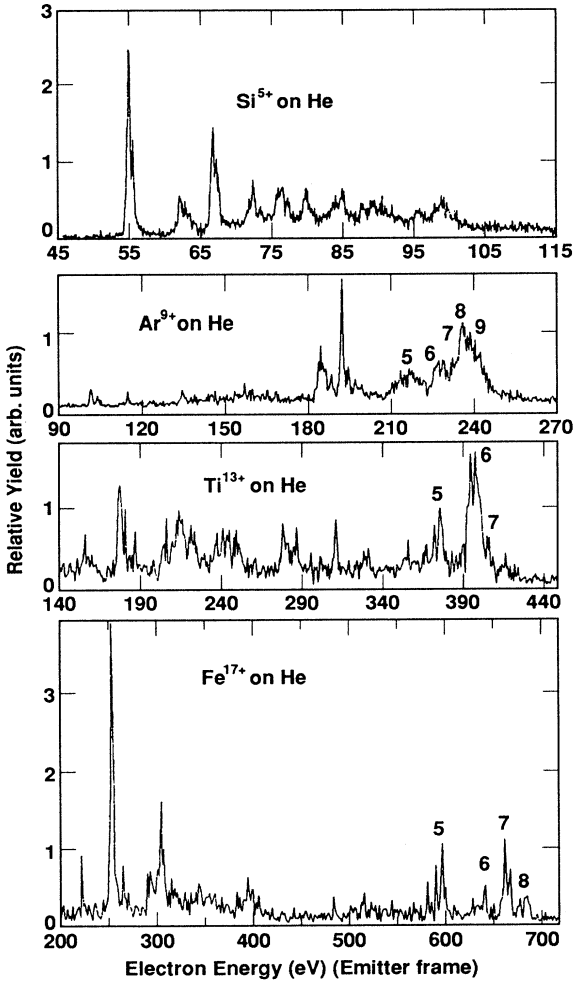

FIG. 3. Auger spectra from F-like Si, Ar, Ti, and Fe colliding on a He-gas cell target. Each spectrum is normalized to a target pressure of 0.3 mTorr. The dwell time at each point was normalized to the charge collected in the Faraday cup. The intensity for each projectile has been divided by the initial projectile charge state for comparison purposes. (Therefore, to normalize to the same number of particles, each of these spectra should be multiplied by the square of the F-like projectile charge.) The most striking feature is the rapid growth of one line in particular as Z increases. This line has been identified as due to the decay of the $2p^5 3s3p\ ^4D_{7/2}$ metastable level. The numbers (5, 6, 7, 8, etc.) refer to the n quantum number in the $2p^5 3snl$ configuration.

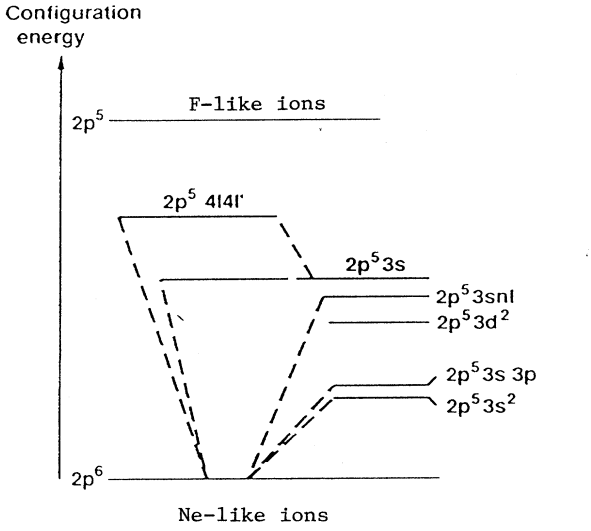

FIG. 4. Energy diagram showing the configuration ordering for Na-like ions. The configurations shown are $2p^5 3snl$ and $2p^5 4l4l'$.

The single-collision double-capture process has, in turn, two different competing mechanisms; these are (a) sequential capture (during a single collision) of two electrons, one at each of two avoided crossings of the relevant molecular-orbital energy levels, (b) the process of two-electron capture at a single avoided crossing.

The concept in (b) of "dynamical" or "scattering correlation" was discussed originally for He-like projectiles (O^{6+}) colliding on a He-gas target [14]. This work provides evidence of similar double-capture behavior for initial projectile ions belonging to the F I sequence.

Mechanisms (a) and (b) are expected to populate different configurations of the final Na-like ion. The sequential capture process (a) should populate configurations such as $2p^5 nln'l'$, where $n' \approx n$ and $l' \approx l$, e.g., $2p^5 3l4l'$, $2p^5 3l3l'$, $2p^5 4l4l'$, and possibly $2p^5 3l5l$ (equivalent or near-equivalent configurations) for the Ar^{9+} case. However, the correlated capture process (b) can lead to the population of highly nonequivalent configurations, e.g., $2p^5 3snl$, where $n > 3$. In [13] it was shown that a peak of the population occurred at around $2p^5 3s8l$ for Ar^{9+} colliding on He (at least for electrons emitted in the beam direction).

Ne-LIKE PROJECTILES

The ground state of Ne-like ions is $2p^6\ ^1S_0$ and single-electron capture to this configuration will not populate Auger levels. Ne-like ions have the two metastable levels $2p^5 3s\ ^3P_0$ and $^3P_2$. The lifetimes of these levels are of some importance as the population is formed in the ECR plasma and the transit time from source to target is $\sim 11-18\ \mu s$.

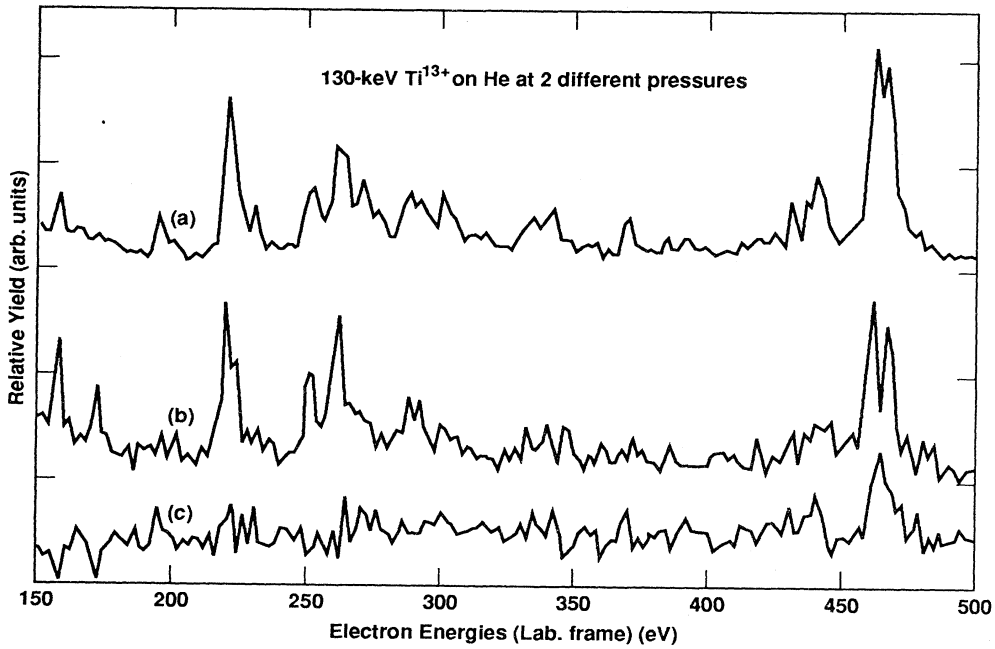

FIG. 5. Pressure scaling of spectra from 130-keV Ti^{13+} colliding with He. Spectrum (a) has been divided by two and was taken at twice the pressure of spectrum (b). Spectrum (c) is the difference (a)−(b). Two electrons each captured in separate collisions would produce intensity features showing a quadratic pressure dependence. This is seen in (c) as the feature near 460 eV and is attributed to decay from $2p^5 3s\,5,6l$ configurations; it is seen that not all of this intensity comes from double collisions. Note that the lower energy lines (e.g., $2p^3 3l3l'$) appear to follow a linear pressure dependence, i.e., they are populated by cascades from levels formed by true double-capture collisions.

Single-electron capture to the $2p^5 3s$ metastable Ne-like levels will produce Na-like core-excited levels, namely $2p^5 3s(^3P_{0,2})nl$. Furthermore, the n, and to some extent the l, quantum numbers in these configurations can be estimated by the semiclassical over-barrier model. In Fig. 6 we show predicted values for n and l from the classical over-barrier model for single-electron capture [8,15]. The n value is given by

$$n^2 = \frac{q^2(2\sqrt{q}+1)}{2I(\sqrt{q}+q)} , \tag{1}$$

where q is the ion charge and I the ionization potential, in a.u., of the target atom. The maximum internuclear separation for electron transfer R_c is given by

$$R_c = \frac{2(q-1)}{-2I+q^2/n^2} . \tag{2}$$

The l value is estimated to be $l \approx m_e v_p R_c/\hbar$, with v_p the projectile velocity. From Eqs. (1) and (2) one has then

$$l \approx \frac{2\sqrt{q}+1}{I} 6.29 \left[\frac{E(\text{MeV})}{M(\text{amu})} \right]^{1/2} , \tag{3}$$

with M and E the projectile mass and kinetic energy.

Yrast levels are those with the maximum $l=n-1$. The maximum j level of an yrast configuration may decay radiatively only down the yrast chain of similar states of lower n and can lead to strong population of low-lying configurations such as $2p^5 3s3p$. This model can be used with care for any isoelectronic sequence—the model depends only on the ion charge, the beam velocity for l, and the ionization potential of the target. A good illustration of the utility of the over-barrier model is found in the collision system of Ar^{8+} on He. The predicted values of n and l are 4 and ~2, respectively; previous electron spectroscopic studies have shown $2p^5 3s4d$ to be the most probable "capture" configuration [16].

The spectra obtained in the present experiments have been analyzed or compared in two ways.

(i) We compare the spectra produced by single-electron capture to the metastable fraction of a Ne-like beam to those produced by double-electron capture to the corresponding F-like beams.

This has been done for the Na-like projectile final states of Si^{3+}, Ar^{7+}, and Ti^{11+} (the $2p^5 3s\ ^3P_2$ lifetime for Ne-like Ti is around 35 μs (beam flight time ~13 μs) and the $^3P_0$ is much longer lived. This comparison is shown in Fig. 7. Here the final Auger configurations are mainly $2p^5 3snl$. The $3s$-$3p$ excitation energy is around 10 eV for Si and thus collisional excitation is not expected to have high probability at these beam energies.

(ii) We compare spectra produced by the different F-like projectile beams. Here isoelectronic regularities and relative cross sections are of interest. Such spectra are

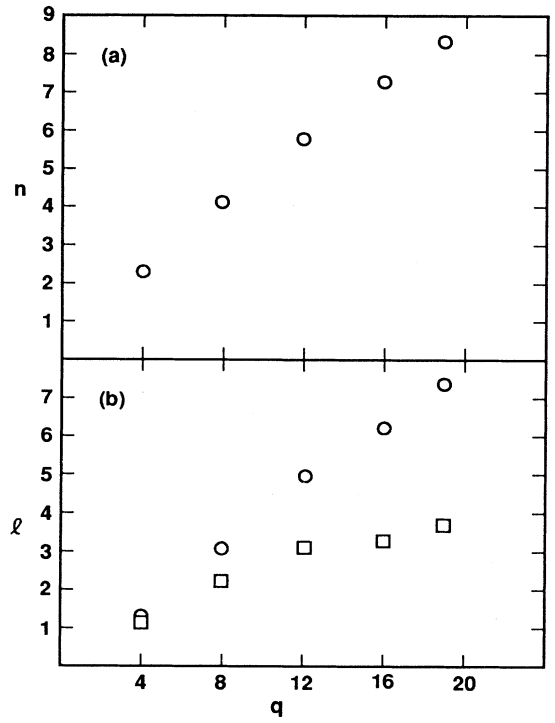

FIG. 6. Predictions of the classical over-barrier model for (a) n and (b) l values (squares) for single-electron capture from a He-gas target. Circles in (b) are the yrast values associated with the predicted n. The model shows that, for highly charged ions, e.g., $q \geq 12$, it is unlikely that yrast levels will be populated at the collision velocities studies here (0.24–0.36 a.u.).

shown in Fig. 3.

It is evident that one single line grows very fast in intensity as the projectile increases. This line has been identified as from the Auger decay of the metastable $2p^5 3s 3p\ ^4D_{7/2}$ level. The integers (5,6,7, . . .) above the spectral lines in Fig. 3 refer to the n quantum number in $2p^5 3snl$. Hydrogenic energy values for these configurations are given in Table I.

The metastability of this level has been discussed in [11] in relation to Na-like Fe, however, some of the details will be repeated here. The $2p^5 3s 3p\ ^4D_{7/2}$ level of Na-like ions is forbidden to decay by Coulomb autoionization or electric dipole ($E1$) photon emission. This is because it is very nearly a pure state of total spin $\frac{3}{2}$ (quartet). There are no lower energy, opposite parity states with the same total spin to which it might decay by $E1$ emission. Similarly, the Auger final state $2p^6 \epsilon l$, with spin $\frac{1}{2}$, cannot be reached because Coulomb autoionization preserves spin. The level does autoionize slowly via the spin-spin part of the Breit interaction to the final state $2p^6 \epsilon l (J = \frac{7}{2})$. The metastability of this line has been established in the various spectra by biassing the He-gas cell as demonstrated in Fig. 4. The lifetime of this level has been calculated by Chen [17] using a multiconfiguration Dirac-Fock (MCDF) approach including contributions from the Breit interaction. These calculations show that the Auger branching ratio is essentially 1 for all ions considered here. There is an $M2$ radiative decay branch to the $2p^6 3s\ ^2P_{3/2}$ which becomes important for the higher-Z ions. Table II contains measured and calculated energies for the Auger line from the $2p^5 3s 3p\ ^4D_{7/2}$ level for a number of Na-like ions.

This level is particularly interesting because (a) its Auger branching ratio is 1 and (b) it is a pure quartet level. Direct population of such a level would require one of the captured electrons to reorient its spin, as the target electrons have opposite spin ($1s^2\ ^1S_0$). The apparent intensity of the $^4D_{7/2}$ line is greatly affected by the variation of the metastable level decay length as the Z of the projectile is charged. Table III lists intensities observed and corrected for the decay length variation for Ar^{7+}, Ti^{11+}, and Fe^{15+} ions, the decay constants being taken

TABLE I. Hydrogenic energies for the yrast levels belonging to the $2p^5 3snl$ configurations $E_n = E_\infty = -13.6(Z_0/n)^2$, where Z_0 is the charge state of the Ne-like ion and E_∞ is the energy of the lowest $2p^5 3s$ level above the $2p^6\ ^1S_0$ Ne-like ground state. This approximation is best for the higher l levels for a given n (i.e., nonpenetrating orbitals), and the accuracy increases with n. The energies in the table are given in eV. The Ar^{7+} energies can be compared to those Folkmann *et al.* [27].

$2p3sn$ $(l = n-1)$	Ar^{7+}	Ti^{11+}	Fe^{15+}
$n=4$	197.6	336.1	507.6
5	217.2	380.2	585.9
6	227.8	404.1	628.4
7	234.2	418.5	654.1
8	238.4	427.9	670.8
9	241.3	434.9	682.2
10	243.3	438.9	690.4
11			696.4
12			701.0
∞	252	458.5	725.2

TABLE II. Measured and calculated energies for the $2p^5 3s 3p\ ^4D_{7/2}$ decay for a number of Na-like ions. The calculated values are taken from [17] and a private communication for Si. The decay was not observed for Si^{3+} as the level lifetime is so long that very little decay occurs along the available 100 mm.

Ion	Measured energy (eV)	Calculated energy[a] (eV)
Si^{3+}	not observed	61.1
Ar^{7+}	114.1(3)	114.1
Ti^{11+}	176.5(5)	178.0
Fe^{15+}	253.9(5)	252.5
Cu^{18+}	312.8(5)	315.1

[a]MCDF plus Breit calculation by Chen [17].

TABLE III. Measured and corrected relative intensities per ion per unit target thickness for the Auger decay of the $2p^5 3s 3p\ ^4D_{7/2}$ metastable level for Na-like Ar^{7+}, Ti^{11+}, and Fe^{15+}.

Ion	q_0	Relative line intensities Measured	Corrected
Ar	9	0.10	0.40
Ti	13	1.00	1.00
Fe	17	7.17	2.95

from [17], and for the change of the spectrometer acceptance solid angle along the ~10-cm decay path following the gas cell. These data suggest that the population of the $2p^5 3s 3p\ ^4D_{7/2}$ level scales at a rate roughly equivalent to the third power of the charge of the F-like ion (q_0). The intensities in Fig. 7 have been divided by the charge of the F-like projectile for convenience of comparison. This scaling turns out to match that of the $2p^5 3s^2\ ^2P$ term if the intensities from the ^2P decays are scaled by the branching ratios for Auger decay. These

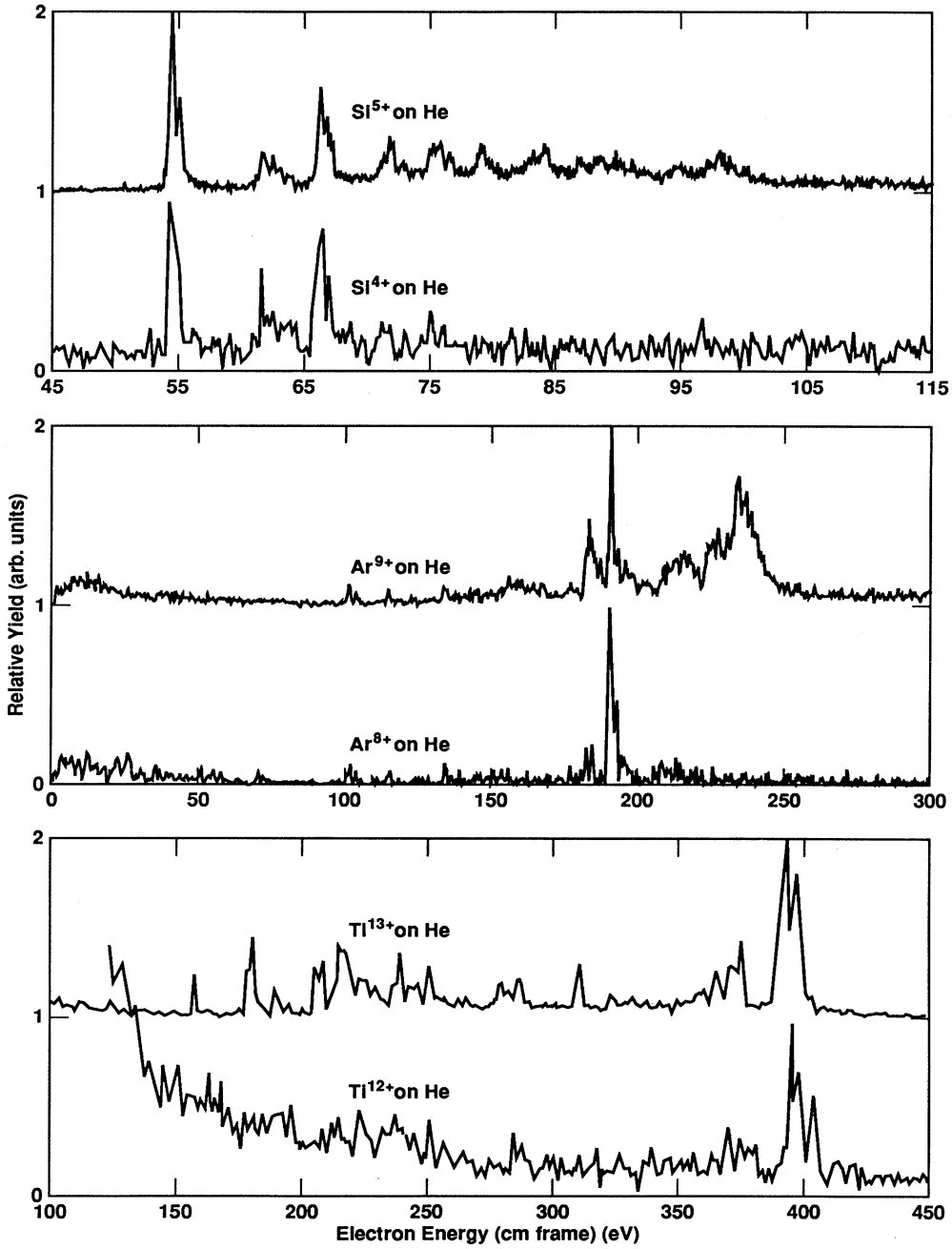

FIG. 7. Comparison of Na-like Auger lines produced by F-like and Ne-like projectiles colliding on He. For each pair, regions of the spectra corresponding exclusively to double-electron capture to the F-like projectile can be seen. All beam energies are 10 keV$\times q$.

branching ratios are also taken from the work of Chen [17]. However, neither of the two mechanisms for double-electron capture predict the population of such low-lying levels, especially considering the strong q_0 dependence. This suggests that these levels are populated by radiative cascades. This argument does not rule out spin reorientation into higher $2p^5 3snl^4(l+1)$ levels; however, the probability for a spin reorientation is small and the present data do not give any support to such a mechanism. One reason for very high population of the $2p^5 3s3p\ ^4D_{7/2}$ is that it is fed directly by the radiative yrast chain, whereas the $3s^2\ ^2P$ term is not. However, cascades may also populate the $2p^5 3s3p\ ^4D_{7/2}$ level in the spectra produced by the Ne-like projectiles.

Figure 6 indicates that Ti^{12+} colliding on He should populate configurations such as $2p^5 3s5l$ (for the metastable beam fraction). Such configurations have energies around 400 eV. Figure 6 also suggests that the l value should be about 3, i.e., smaller than the maximum allowed ($l=4$). Thus the yrast levels may not be significantly populated. It is known from work at higher beam energies using a carbon foil for excitation that the decay of yrast levels leads to strong population of low-lying configurations [18]. However, high-n levels off the yrast branch have, in general, higher x-ray and Auger branching ratios and this may explain the apparent low intensity of the $2p^5 3s3p\ ^4D_{7/2}$ decay in Fig. 7. It should be pointed out here that a proper comparison of the Auger intensities for the Ne-like and F-like beams colliding on He is hindered by an incomplete knowledge of the fraction of the Ne-like beams in the metastable ($2p^5 3s\ ^3P_{0,2}$) levels. Methods of measuring or estimating the metastable beam fractions of ECR beams have been discussed, e.g., Ref. [19]; usually these methods are based on optical spectroscopy. In general, the metastable beam fraction will depend on the particular element being extracted from the ion source and also which charge state has been optimized. In Fig. 8 we show the charge states produced by the LBL ECR for Ar and Ti as the source was run for the experiments reported here. It may be that the $2p^5 3s\ ^3P_{0,2}$ metastable beam fractions were greater for Ar^{8+} than for Ti^{12+}, as is evident from Fig. 8. The figure shows ECR beam current for the different charge states plotted against the energy to reach charge state q from $q-1$.

The double-capture mechanism appears to lead to population of highly nonequivalent configurations. This is similar to the findings of Ref. [14] and also shows some similarity to the bound-continuum capture work of Tanis *et al.* [20]. It would appear that the two electrons (captured to a bound configuration) "repel" each other in both n and l space, leading to population of levels on or close to the yrast chain. Similar population of high-l levels was seen in the collision of 60-keV O^{6+} on He [14]. This could explain the strong population of low-lying levels such as the $2p^5 3s3p\ ^4D_{7/2}$ by cascade repopulation. A high-l population has also been recently seen by observing the yrast transitions following multielectron capture in $Kr^{18+}+Kr$, and $Kr^{18+}+Ar$ collisions by Martin *et al.* [21]. As seen from Fig. 6, single-electron capture is not expected to populate such high angular momentum configuration, at least at these beam velocities. In the spectrum of Ti^{12+} on He the over-barrier model would predict population of the $2p^5 3s(5,6d,f)$ configurations

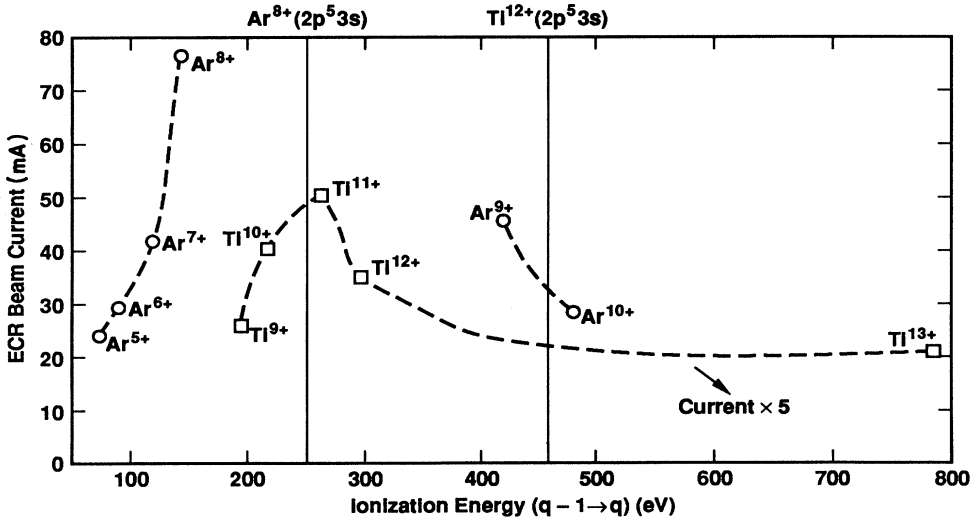

FIG. 8. Beam-currents extracted from the LBL ECR are plotted against the electron energy required to reach each charge state from the preceding one, i.e., $I(q)$ vs $E(q-1\rightarrow q)$. This is done for Ar and Ti extracted under the ECR conditions used in the experiment. Note that the Ti value must be divided by 5 to get the true beam current. The vertical lines show the excitation energy of the metastable Ne-like configurations above the $2p^6$ ground state.

which are off the yrast chain. The energy of such configurations is around 380–410 eV; see Fig. 7. However, as in Ref. [13], we might expect that the population of the $2p^5 3s5,6d$ configurations would show a quadratic pressure dependence for the Ti^{13+} on He system. In our pressure-dependence studies, Fig. 5, we found less evidence for this than in the $Ar^{9+,8+}$ comparison [13]. However, clearly some of the higher $2p^5 3snl$ energy lines show a greater than linear pressure dependence. The less convincing nature of this process may be explained by the following.

(a) The double-electron-capture process may dominate over single-electron capture for such highly charged projectiles at these low velocities. The double-capture process could, of course, also populate other configurations decaying with the same energy, within the resolution of the system. We cannot resolve decays from $2p^5 3snl$ or $2p^5 3snl'$ for large values of n. In [22] it was found that multielectron capture in $Ar^{q+}+Ar$ collisions accounted for a large percentage of the total capture cross section. Reference [23] also shows a larger cross section for double-electron capture compared to single capture.

(b) The configurations populated in the single-capture–two-collision process should have a lower total angular momentum than that of the true double-electron-capture case. This may lead to population of levels with higher x-ray branching ratios and therefore less Auger intensity. The x-ray branching ratio increases strongly with increasing Z.

The picture constructed here is based only on the lines seen in the spectra. It is clear from Ref. [17] that the x-ray and Auger transition probabilities do not scale in an ordered manner, at least for the $3l3l'$ configurations. In general, the x-ray fluorescence yield increases with Z, but this is not true for all levels, e.g., $2p^5 3s3p\ ^4D_{5/2}$, where a decrease is predicted for the elements studied here ($14 < Z < 29$). It should also be noted that each level has in fact three decay branches: (i) x-ray transitions to the $2p^6 nl$ closed core configuration, (ii) Auger transitions (strongest to the nearest continuum), and (iii) photon transitions within the core-excited system itself. This latter branch may be of some importance for the higher-Z ions especially for those levels with low x-ray and Auger rates, i.e., yrast and near-yrast levels. Lifetime measurements of some $3l3l'$ levels for S and Cl are being carried out by Jupén and co-workers following a spectral analysis of the core-excited configurations of Na-like, S, Cl, Ar, and Ti [24,25].

These experiments have been conducted at a constant extraction potential of 10 kV and it is conceivable that the results would vary significantly with beam velocity. One study of the velocity dependence of the total double-capture cross section [23] shows that this cross section is, however, less sensitive to the beam velocity than the single-capture cross section, although for individual levels cross sections can be strongly dependent on the beam velocity [26]. We have only also studied electrons emitted at 0°, i.e., along the beam direction and strong anisotropies have been recently observed in double-capture collision [26].

An interesting effect of using odd-Z nuclei is shown in Fig. 9. This shows Auger spectra produced by F-like Sc^{12+} and Cu^{20+} colliding on He. The spectra are normalized in the same way as those shown in Fig. 3. Although similar to Ti and Fe regarding the configurations populated, there is a striking difference in the overall intensity. The drop in intensity may be due to hyperfine mixing of the Auger levels with levels having strong x-ray transitions. It may be that the hyperfine interaction will quench to some extent the population of metastable beam components. Another interesting side issue is the appear-

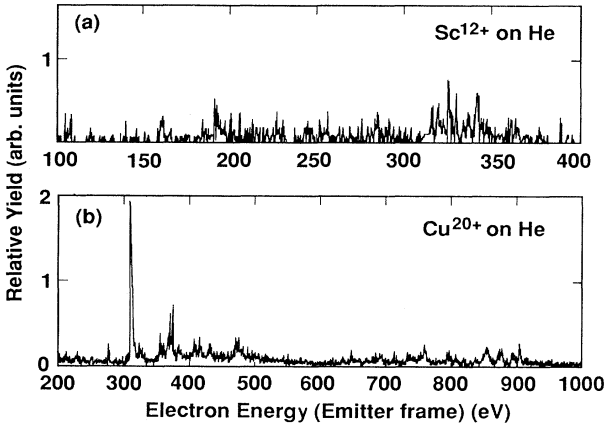

FIG. 9. Spectra produced by F-like Sc and Cu colliding on He normalized in the same way as Fig. 3. The loss of Auger intensity may be caused by hyperfine quenching of the Auger levels. However, the general trends shown by these spectra as to which configurations are populated are similar to those of Fig. 3.

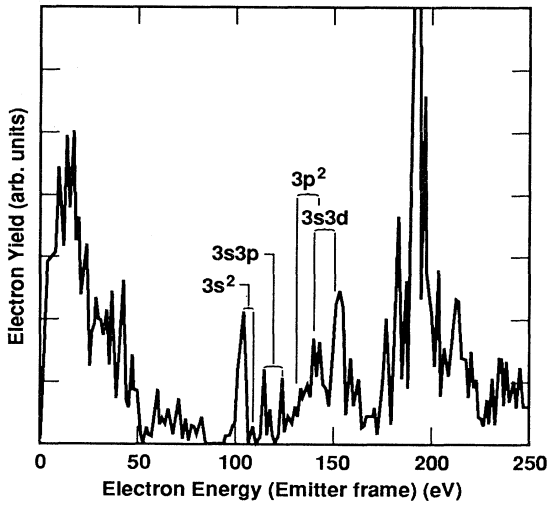

FIG. 10. Auger spectrum produced by 80-keV Ar^{8+} on He shows that configurations such as $2p^5 3p^2$ are populated by $2p^5 3s\ ^3P_{0,2}$ levels capturing one electron. This is due to configuration mixing between $2p^5 3s3d$ and $2p^5 3p^2$, which is strong for all ions in the Na sequence. Note that sd-p^2 mixing is one of the most common interactions in atomic systems.

ance of static atomic correlation in the population of electronic configurations by electron capture. Figure 10 shows in detail the region of spectrum containing the decay of the $2p^5 3l 3l'$ configurations of Na-like Ar. This spectrum is for the system Ar^{8+} on He, i.e., capture of one electron to the $2p^5 3s\ ^3P_{0,2}$ metastable levels of the beam. The $2p^5 3p^2$ configuration is seen to be populated. This should be expected as the $2p^5 3p^2$ and $2p^5 3s 3d$ configurations are quite strongly mixed by configuration interaction. Level energies have been taken from the work of Bengtsson *et al.* [24].

CONCLUSION

We have recorded Auger spectra corresponding to the decay of Na-like core-excited configurations of Si^{3+}, Ar^{7+}, Sc^{10+}, Ti^{11+}, Fe^{15+}, and Cu^{18+}. These configurations have been populated by double-electron capture to beams of F-like ions and for Si, Ar, and Ti by single-electron capture to the metastable fraction of the Ne-like beam. We have observed the population of "non-equivalent" configurations (i.e., $2p^5 3s 6l$, $3s 7l$, etc.) by the double-capture mechanism. This is similar to the results of Stolterfoht *et al.* [14] for 60-keV O^{6+} on He. Evidence for cascade population of the lower-lying configurations ($2p 3s 3l$) is presented, in particular cascade population along the yrast chain. Configuration interaction has been seen to populate $2p^5 3p^2$ when the $2p^5 3s 3d$ configuration is populated (via p^2-sd mixing). The hyperfine interaction has been proposed to both quench the metastable beam fraction from the ECR source and to lessen the Auger intensity (i.e., increase the x-ray fluorescence yield) for odd-Z Na-like ions.

ACKNOWLEDGMENTS

This work was performed under the auspices of the U.S. Department of Energy by the Lawrence Livermore National Laboratory under Contract No. W-7405-ENG-48. Support at LBL was obtained from the Director, Office of Energy Research, Office of Basic Energy Sciences, Chemical Sciences Division, U.S. Department of Energy under Contract No. DE-AC03-76SF00098. We would like to acknowledge Dr. C. F. Moore for providing the McPherson analyzer used in these experiments.

*Present address: Manne Siegbahn Institutet för Fysik, Fresgativ 24, S-104 05 Stockholm, Sweden.

[1] N. Stolterfoht, Phys. Rep. **146**, 315 (1987).
[2] E. D. Donnets, Phys. Scr. **T3**, 11 (1983).
[3] R. Geller and B. Jacquot, Phys. Scr. **T3**, 19 (1983).
[4] J. Arianer, A. Cabrrespine, and C. Goldstein, Nucl. Instrum. Methods **193**, 401 (1982).
[5] D. Schneider, D. DeWitt, M. W. Clark, R. Schuch, C. L. Cocke, R. Schmieder, K. J. Reed, M. H. Chen, R. Marrs, M. Levine, and R. Fortner, Phys. Rev. A **42**, 3889 (1990).
[6] R. K. Janev and H. Winter, Phys. Rep. **117**, 265 (1985).
[7] C. M. Lynesis (unpublished).
[8] H. Ryufuku, K. Sasaki, and T. Watanabe, Phys. Rev. A **21**, 745 (1980); R. Mann, F. Folkmann, and H. F. Beyer, J. Phys. B **14**, 1161 (1981).
[9] D. J. Clark, C. M. Lynesis, M. H. Prior, R. G. Stokstad, S. Chantrenne, and P. O. Egan, in Proceedings of the Tenth Conference on Applications of Accelerators in Research and Industry, Denton, 1988 [Nucl. Instrum. Methods Phys. Res. Sec. B **40/41**, 6 (1989)].
[10] N. Stolterfoht, A. Itoh, D. Schneider, Th. Schneider, G. Schieietz, H. Platten, G. Nolte, R. Glodde, U. Stettner, W. Zeitz, and T. M. J. Zouros, in *International Conference on X-Ray and Inner-Shell Processes in Atoms, Molecules, and Solids, Invited Lecture,* edited by A. Meisel (University Press, Leipzig, 1983).
[11] D. Scheider, M. H. Chen, S. Chantrenne, R. Hutton, and M. H. Prior, Phys. Rev. A **40**, 4313 (1989).
[12] D. Schneider, N. Stolterfoht, G. Schiwietz, T. Schneider, W. Zeitz, R. Bruch, and K. T. Chung, Nucl. Instrum. Methods Phys. Res. Sect. B **24-25**, 173 (1987).
[13] R. Hutton, M. H. Prior, S. Chantrenne, M. H. Chen, and D. Schneider, Phys. Rev. A **39**, 4902 (1989).
[14] N. Stolterfoht, C. C. Havener, R. A. Phaneuf, J. K. Swensen, S. M. Shafroth, and F. W. Meyer, Phys. Rev. Lett. **57**, 74 (1986); F. W. Meyer, D. C. Griffin, C. C. Havener, M. S. Hug, R. A. Phaneuf, J. K. Swenson, and N. Stolterfoht, Phys. Rev. Lett. **60**, 1821 (1988).
[15] J. Burgdörfer, R. Morgenstern, and A. Niehaus, Nucl. Instrum. Methods Phys. Res. Sect. B **23**, 120 (1987).
[16] A. Bordinave-Montesquieu, P. Benoit-Cattrin, M. Boudjema, A. Gleizer, and S. Douson, Nucl. Instrum. Methods Phys. Res. Sect. B **23**, 94 (1987).
[17] M. H. Chen, Phys. Rev. A **40**, 2365 (1989).
[18] W. L. Wiese and S. M. Younger, J. Phys. Colloq. (Paris) **1**, C1-146 (1979).
[19] M. Druetta, S. Martin, and J. Desesquelles, in Proceedings of the Conference on Physics of Multiply Charged Ions, Groningen, 1986 [Nucl. Instrum. Methods Phys. Res. B **23**, 268 (1987)].
[20] J. A. Tanis, D. Schneider, S. Chantrenne, M. H. Prior, R. Herrman, R. Hutton, and G. Schiwietz, Phys. Rev. A **42**, 5776 (1990).
[21] S. Martin, A. Denis, Y. Ouerdane, A. Salmoun, A. El Motassadeq, J. Désesquelles, M. Druetta, D. Church, and T. Laony, Phys. Rev. Lett. **64**, 2633 (1990).
[22] L. Liljeby, G. Astner, A. Bárány, H. Cederquist, H. Darared, S. Huldt, P. Hvelplund, A. Johnson, H. Knudsen, and K.-G. Rensfeldt, Phys. Scr. **33**, 310 (1986).
[23] K. Soejima, K. Okuno, and Y. Kaneko, in *Proceedings of the 16th International Conference on the Physics of Electronic and Atomic Collisions, New York, 1989,* AIP Conf. Proc. No. 205, edited by A. Dalgarno, R. S. Freund, M. S. Lubell, and T. B. Lucatorto (AIP, New York, 1990).
[24] P. Bengtsson, L. Engström, C. Jupén, and M. Westerlind, University of Lund Atomic Spectroscopy Year Report, 1989, p. 14.
[25] C. Jupén, L. Engström, R. Hutton, N. Reistad, and M.

Westerlind, Phys. Scr. (to be published).
[26] R. A. Holt, M. H. Prior, K. L. Randall, R. Hutton, J. McDonald, and D. Schneider, Phys. Rev. A **43**, 607 (1991).
[27] F. Folkmann, K. M. Cramon, R. Mann, and H. F. Beyer, Phys. Scr. **T3**, 166 (1983).
[28] C. Jupén, L. Engström, R. Hutton, and E. Träbert, J. Phys. B **21**, L347 (1988).